

Low-temperature oxidation study of the oxidation of a long chain aldehyde: *n*-hexanal

Anne Rodriguez, Olivier Herbinet, Frédérique Battin-Leclerc

Laboratoire Réactions et Génie des Procédés, CNRS-Université de Lorraine, 1 rue Grandville, 54000 Nancy, France

Supplementary Material

Summary

Description of analytical methods:.....	2
Gas chromatography:.....	2
Cavity ring down spectroscopy:	3
Mole fraction profiles not shown in the main text	5
Reaction added for the hexanoyl radical (R29C6H11OK).....	6
Flow rate analysis	7
Comparison of literature kinetic constants.....	8
“H-atom abstraction by OH” kinetic constants:	8
“H-atom abstraction by HO ₂ ” kinetic constants:.....	9
Sensitivity analyses at 650 K.....	10
References.....	12

Description of analytical methods:

Gas chromatography:

Three gas chromatographs were used for the quantification of the range of products from methane up to C₆ species. All devices were fitted with sampling valves for online injections. The volume of injection loops was 250 µL.

The first one was equipped with a carbosphere packed column and a thermal conductivity detector. It was used for the quantification of O₂, CO and CO₂, with a detection limit of about 100 ppm. The carrier gas was helium. The oven temperature profile was 10 min at 303 K, 5 K/min up to 473 K and a final 16 min isotherm.

The second gas chromatograph was equipped with a PlotQ capillary column and a flame ionization detector for the quantification of C₁-C₅ species. The flame ionization detector was preceded by a methanizer enabling the detection of species containing carbonyl functions with a better sensitivity (detection limit in the range 1-10 ppm depending on species). Note that the detection of formaldehyde by gas chromatography was possible but that the uncertainty in mole fractions is relatively high (estimated to ±20%, compared to ±5% for other species) due to very tailing peaks in chromatograms and coelution. Formaldehyde could be quantified with a better accuracy using cw-CRDS. The carrier gas flow rate (helium) was held constant at 2 mL/min. The oven temperature profile was 10 min at 333 K, 5 K/min up to 523 K and a final 15 min isotherm.

A third gas chromatograph was equipped with an HP5 capillary column and a flame ionization detector for the quantification of species having more than 6 carbon atoms. Carrier gas (helium) flow rate was held constant (1 mL/min) and the temperature profile of the oven was: 15 min at 313 K, 5 K/min up to 473 K and a 8 min final isotherm.

Another gas chromatograph coupled to a mass spectrometer (with electron impact at 70 eV) was used for the identification of species. Analyses were carried out with HP5 or PlotQ capillary column to obtain the same chromatograms as those obtain with gas chromatographs used for the quantification enabling direct comparisons.

Cavity ring down spectroscopy:

Continuous wave cavity ring down spectroscopy (cw-CRDS) is a technique which relies on the absorption of species: in the present work the near infrared range (6620-6644 cm^{-1}) has been considered. This technique was already successfully used for the detection of several species formed in the oxidation of methane and *n*-butane in a jet-stirred reactor [1–3]. In the present study, cw-CRDS was used for the quantification of water, formaldehyde and hydrogen peroxide. The measurement cell is composed of a glass tube with a cavity formed by two highly reflective mirrors fixed at each extremity of the cell. One of the two mirrors is fixed to a piezo actuator enabling the periodic modulation of the cavity length in order to obtain resonance between the wavelength and the cavity modes. A diode laser beam enters the cell through one mirror and the signal exiting through the other mirror after many round trips was recorded using an avalanche photo-diode. When the cavity length comes into resonance with the laser light, the recorded signal increases and exceeds a user defined threshold. At this moment, a homemade threshold circuit triggers an acousto-optical modulator and the laser beam was deviated. The decay signal was subsequently recorded as a function of time and the ring-down time is obtained by fitting the exponential decay over a time range of seven lifetimes by a Levenberg-Marquardt exponential fit [1]. 50 ring-down events are typically averaged before incrementing the wavelength of the diode by 0.03 cm^{-1} . The concentration of a species being formed or consumed during the hydrocarbon oxidation process in a jet-stirred reactor (JSR) can be obtained using equation (1).

$$\alpha = [A] \times \sigma = \frac{R_L}{c} \left(\frac{1}{\tau} - \frac{1}{\tau_0} \right) \quad (1)$$

where σ is the absorption cross section, R_L is the ratio between the cavity length L , i.e. the distance between the two cavity mirrors to the length L_A over which the absorber is present, c is the speed of light, τ is the ring down time measured during an experiment, and τ_0 is ring-down time measured under non-reactive conditions.

Absorption lines and cross sections used for the quantification of formaldehyde, water and hydrogen peroxide are given in Table S1. Mole fractions were calculated using two different absorption lines for each species to check the consistency of the data. The line at 6641.67 cm^{-1} for formaldehyde was used at low temperature only because at high temperature this line is too close to one line for H_2O . Note that uncertainties in mole fractions are mainly due to uncertainties in cross sections and in measured ring down times. The average uncertainty in mole fractions was estimated to an average of $\pm 15\%$ depending on the absorption line and the species concentration. The uncertainties in water mole fractions are larger at high temperatures due to the huge

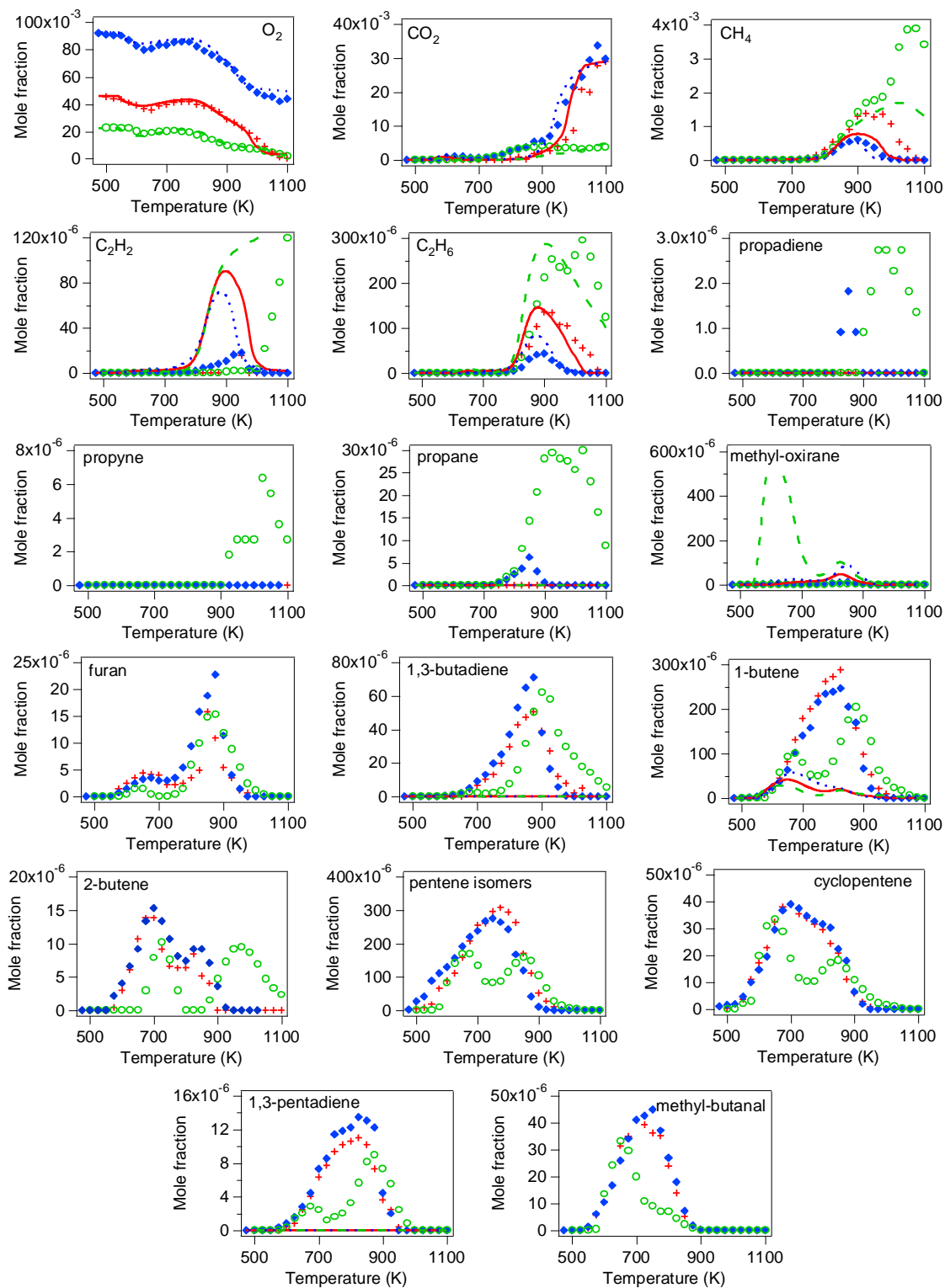
concentration of this species in the cell which eventually leads to line saturation above 850 K. The detection limit depends on the intensity of the absorption line (about 500 ppm here).

Table S1: Absorption lines and cross sections used for the quantification of formaldehyde, water and hydrogen peroxide.

	wavenumber ν (cm^{-1})	cross section σ (cm^2)	reference
CH ₂ O	6639.33	3.60×10^{-22}	Morajkar et al. [4]
	6641.67	4.59×10^{-22}	
H ₂ O	6638.9*	4.46×10^{-23}	Macko et al. [5]
	6640.9	1.60×10^{-22}	
	6641.27*	1.82×10^{-22}	
H ₂ O ₂	6639.26	7.62×10^{-23}	Parker et al. [6]
	6640.06	1.41×10^{-22}	

* These lines were used only at high temperature because they were perturbed by another peak at low-temperature resulting in uncertainties.

Mole fraction profiles not shown in the main text



5

Figure S1: Mole fraction profiles not shown in the main text. Blue: $\phi = 0.5$, red: $\phi = 1$ and green: $\phi = 2$.

Reaction added for the hexanoyl radical (R29C6H11OK)

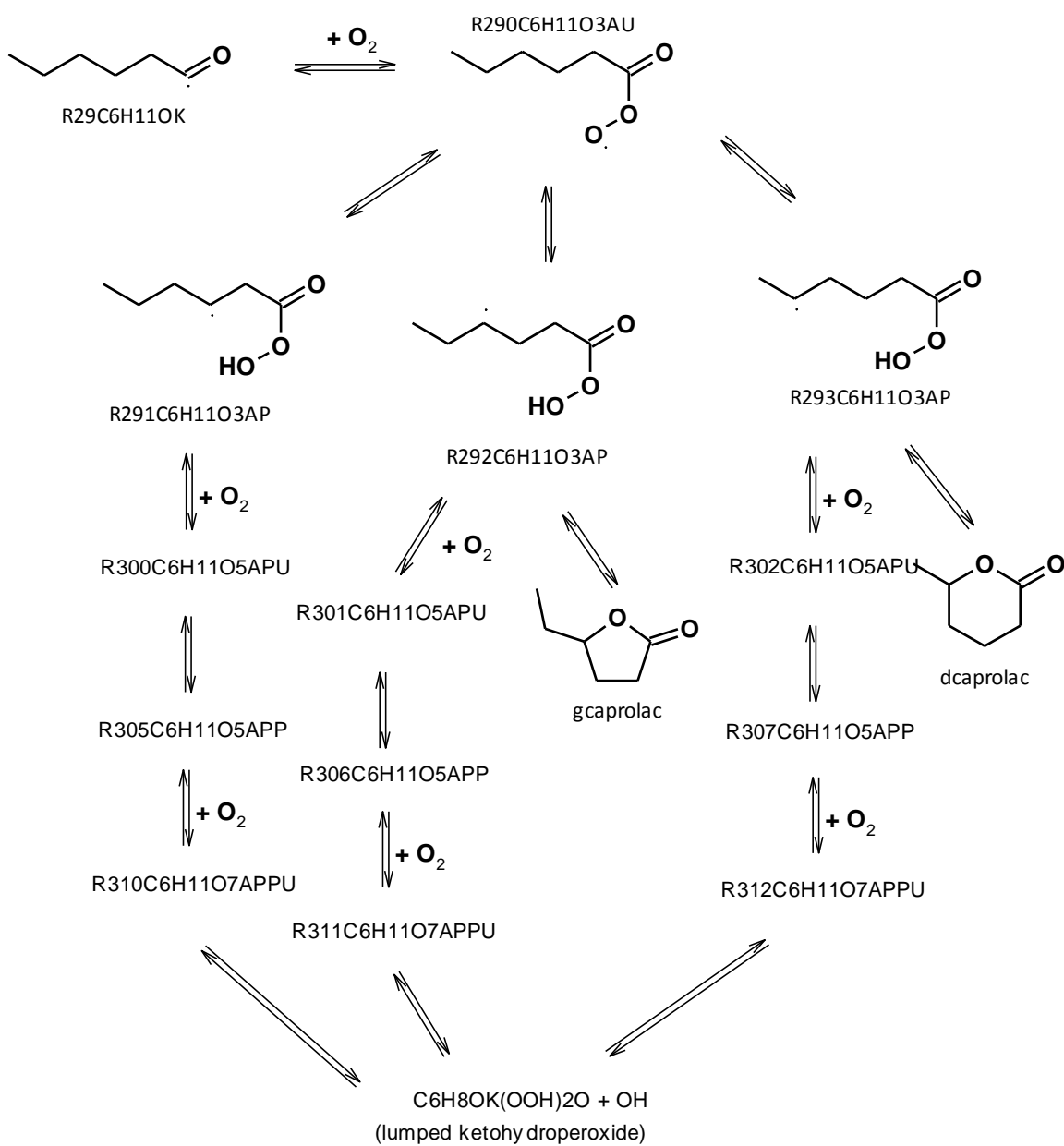


Figure S2: Reactions added for the low-temperature oxidation chemistry of the hexanoyl radical.

Flow rate analysis

Flow rate analysis at 625 K (under stoichiometric conditions) showing that finally 88% of the fuel (C₆H₁₂O_A-1) goes to the hexanoyl radical (R₂₉C₆H₁₁O_K) through isomerizations of fuel radicals.

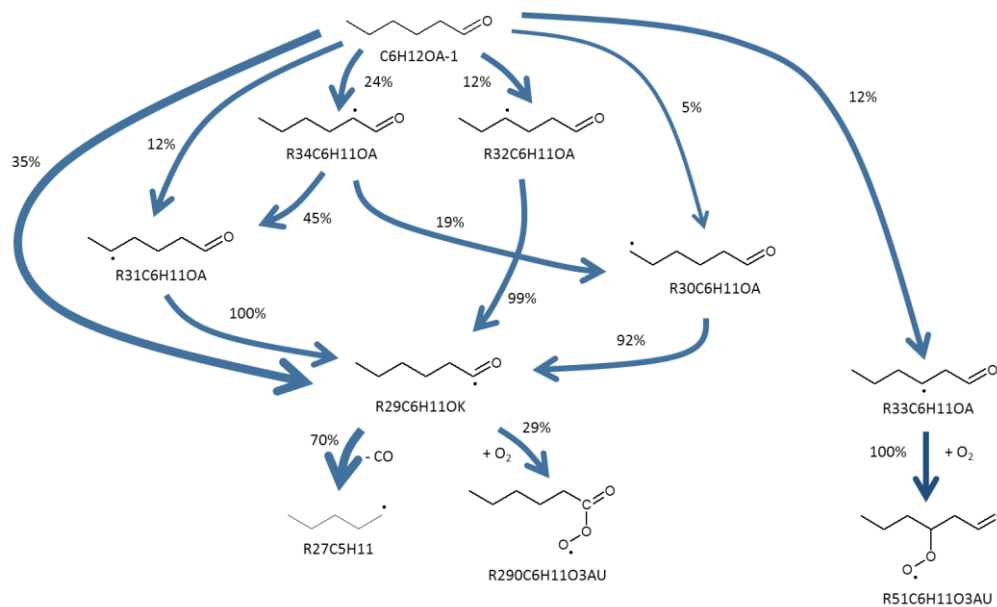


Figure S3: Rate of production analysis performed at 625 K (stoichiometric condition).

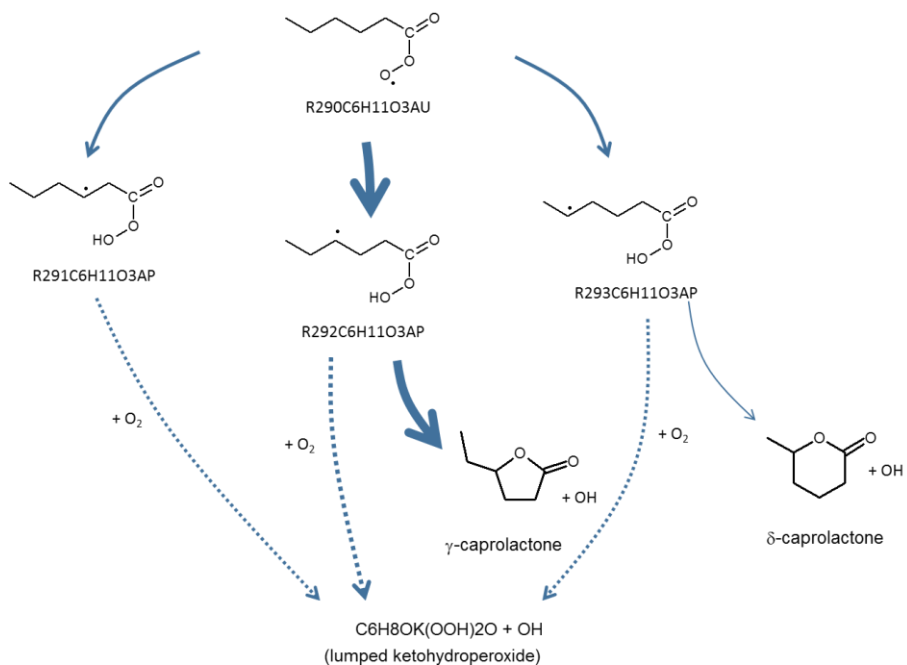
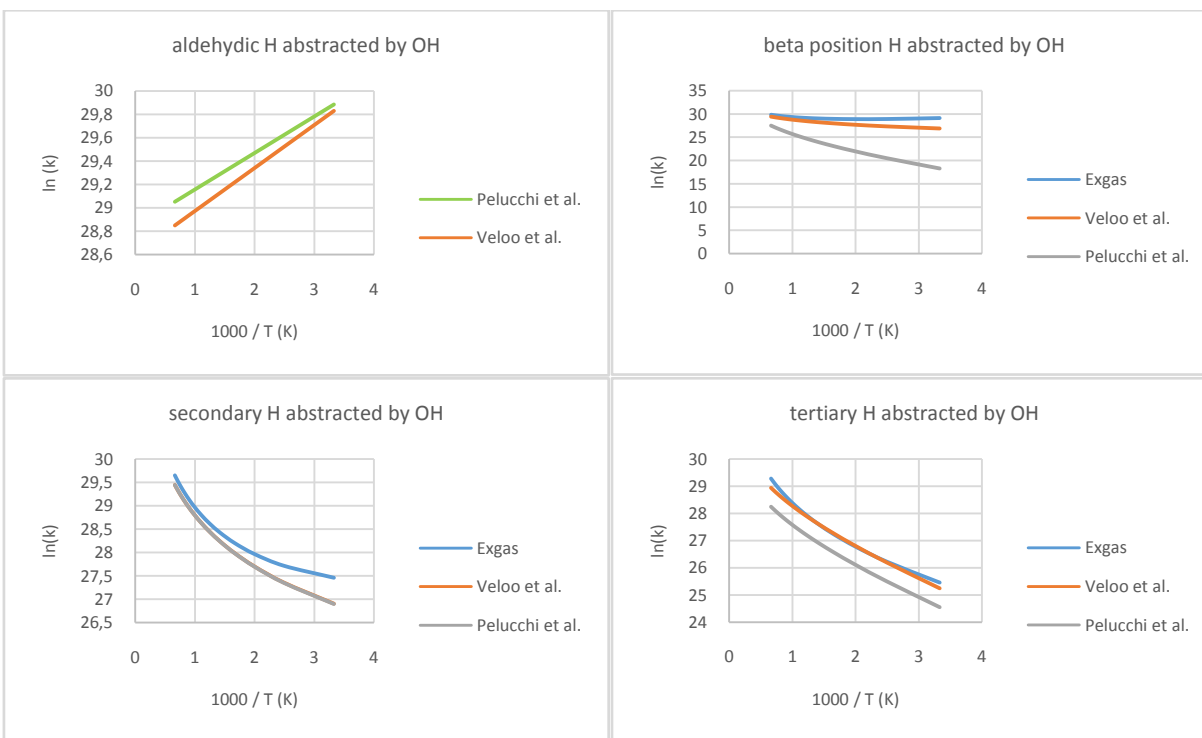


Figure S4: Rate of production analysis performed at 625 K (stoichiometric condition).

Comparison of literature kinetic constants

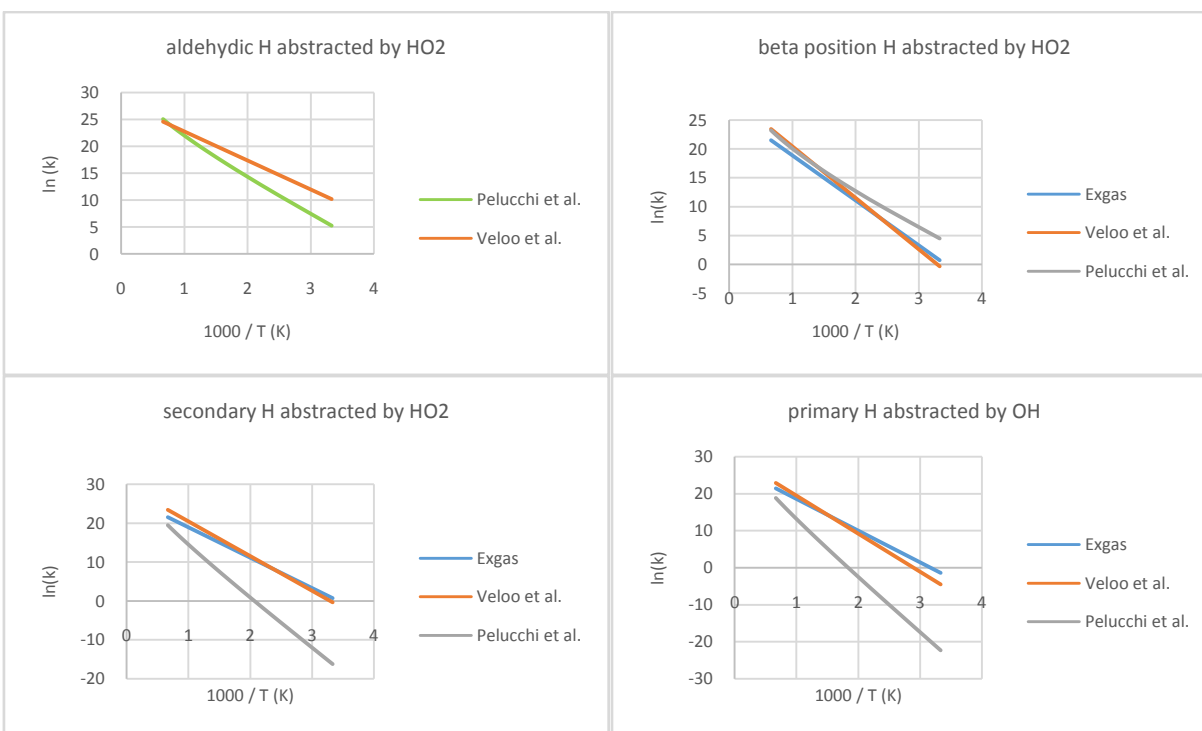
“H-atom abstraction by OH” kinetic constants:



For the aldehydic H-atom, the values used in Nancy are not shown because they are those proposed by Pelucchi et al. [7].

For the beta position, the values used in the present model (Nancy) is that of an H abstraction by OH for a tertiary H-atom. That used by Veloo et al. [8] is the same as that for an H abstraction by OH for a secondary H-atom.

“H-atom abstraction by HO₂” kinetic constants:



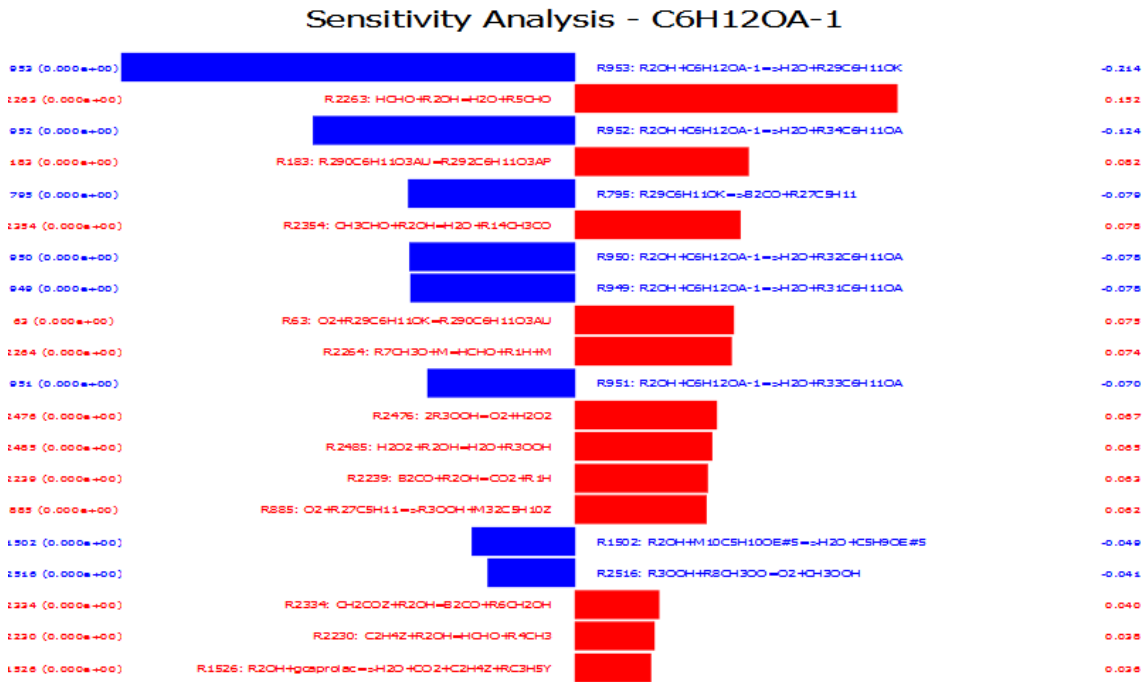
For the aldehydic H-atom, the values used in Nancy are not shown because they are the same as those proposed by Pelucchi et al. [7].

For the beta position, the values used in the present model (Nancy) is that of an H abstraction by HO₂ for a secondary H-atom. That used by Veloo et al. [8] is the same as that for an H abstraction by HO₂ for a secondary H-atom. For abstractions by HO₂, this assumption seems not to bad given the agreement with the kinetic constants proposed by Pelucchi et al. [7].

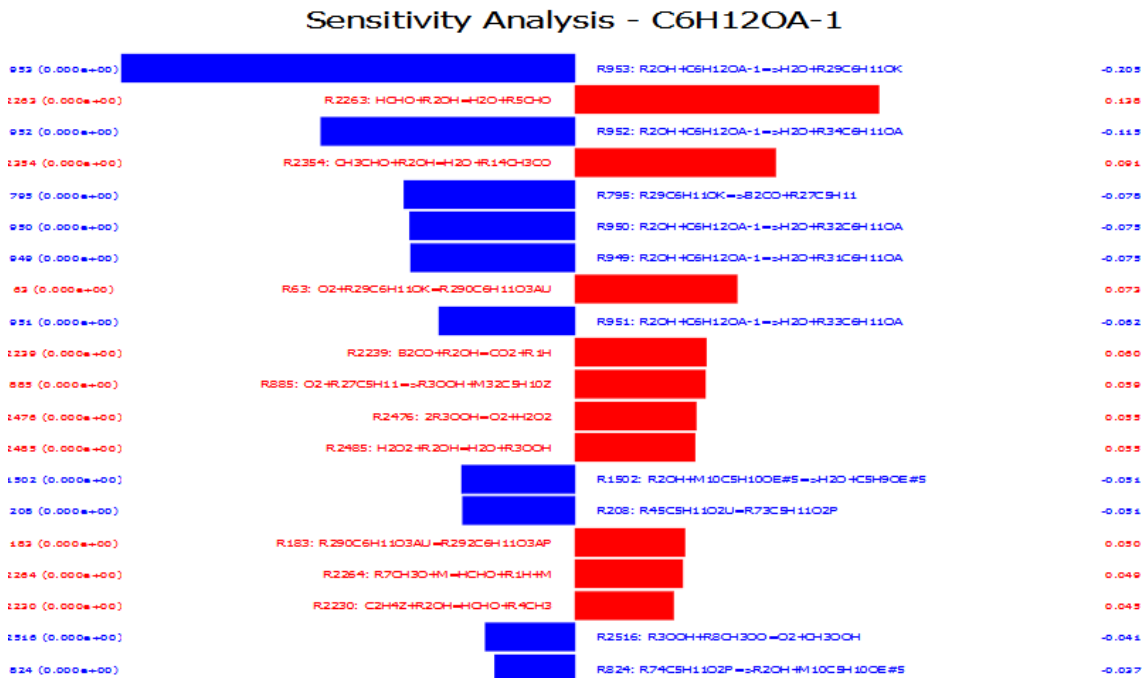
Sensitivity analyses at 650 K

Sensitivity analyses were performed using Opensmoke++ [9,10].

- $\phi = 0.5$

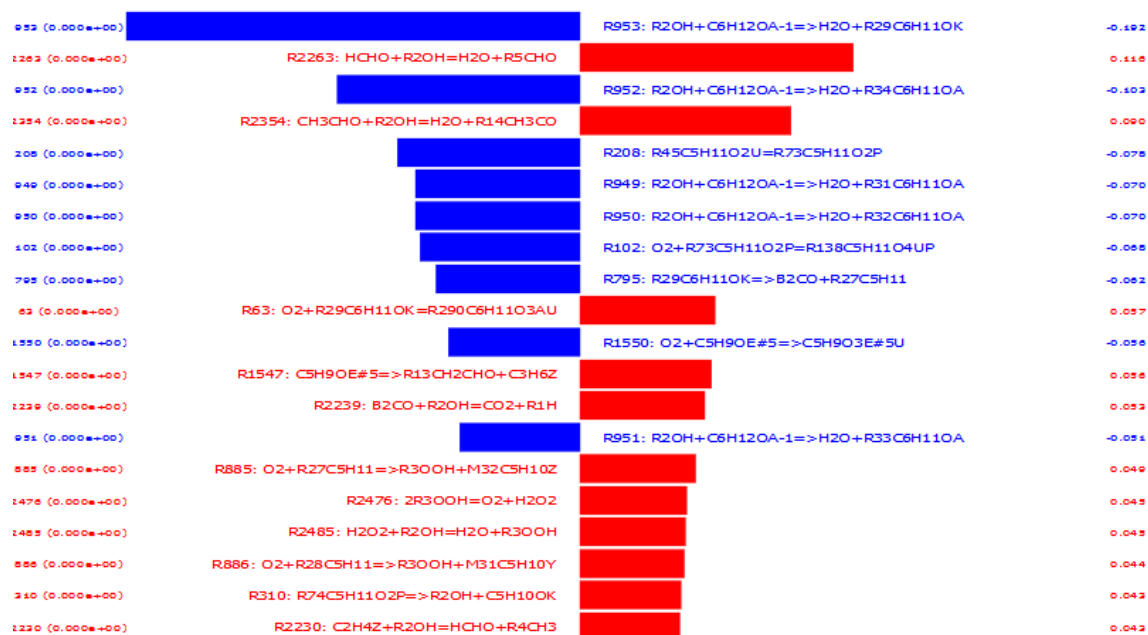


- $\phi = 1$

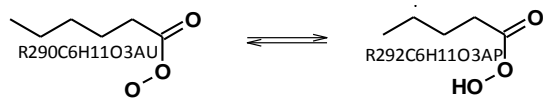


- $\varphi = 2$

Sensitivity Analysis - C6H12OA-1



According to the sensitivity analyses performed at 650 K, one of the main difference between $\varphi = 0.5$ and $\varphi = 1$ is the reaction R183:



which has an inhibitive effect at $\varphi = 0.5$ but not at $\varphi = 1$.

When comparing $\varphi = 1$ and $\varphi = 2$, it appears that the low-temperature chemistry of the *n*-pentyl radical (R208) is more important at $\varphi = 2$ (accelerating effect).

As far as H-atom abstractions are concerned, there are no major difference between the three equivalence ratio. These reactions are likely not responsible for the discrepancies observed at low-temperature.

To sum up, the discrepancies observed at low-temperature at $\varphi = 0.5$ and $\varphi = 2$ are likely due to the low-temperature chemistry of *n*-pentyl and hexanoyl radicals, confirming that more attention is to be paid to these reactions.

References

- [1] C. Bahrini, O. Herbinet, P.-A. Glaude, C. Schoemaeker, C. Fittschen, F. Battin-Leclerc, *Chem. Phys. Lett.* 534 (2012) 1–7.
- [2] C. Bahrini, O. Herbinet, P.-A. Glaude, C. Schoemaeker, C. Fittschen, F. Battin-Leclerc, *J. Am. Chem. Soc.* 134 (2012) 11944–11947.
- [3] C. Bahrini, P. Morajkar, C. Schoemaeker, O. Frottier, O. Herbinet, P.-A. Glaude, F. Battin-Leclerc, C. Fittschen, *Phys. Chem. Chem. Phys.* 15 (2013) 19686–19698.
- [4] P. Morajkar, C. Schoemaeker, C. Fittschen, *J. Mol. Spectrosc.* 281 (2012) 18–23.
- [5] P. Macko, D. Romanini, S.N. Mikhailenko, O.V. Naumenko, S. Kassi, A. Jenouvrier, V.G. Tyuterev, A. Campargue, *J. Mol. Spectrosc.* 227 (2004) 90–108.
- [6] A.E. Parker, C. Jain, C. Schoemaeker, P. Szriftgiser, O. Votava, C. Fittschen, *Appl. Phys. B Lasers Opt.* 103 (2011) 725–733.
- [7] M. Pelucchi, K.P. Somers, K. Yasunaga, U. Burke, A. Frassoldati, E. Ranzi, H.J. Curran, T. Faravelli, *Combust. Flame* 162 (2015) 265–286.
- [8] P.S. Veloo, P. Dagaut, C. Togbé, G. Dayma, S.M. Sarathy, C.K. Westbrook, F.N. Egolfopoulos, *Combust. Flame* 160 (2013) 1609–1626.
- [9] A. Cuoci, A. Frassoldati, T. Faravelli, E. Ranzi, *Comput. Phys. Commun.* 192 (2015) 237–264.
- [10] A. Cuoci, A. Frassoldati, T. Faravelli, E. Ranzi, *Combust. Flame* 160 (2013) 870–886.